Progress in Computer-Aided Manufacturing of Laminated Engineering Materials Utilizing Thick, Tangent-Cut Layers

Yong Zheng[1], Sangeun Choi[2], Brian Mathewson[3], and Wyatt Newman[4]

Abstract

This paper presents recent progress in extending the CAM-LEM process to 5-axis laser cutting for fabrication of laminated engineering components directly from sheet materials. The present extensions enable construction of layered objects from thicker layers by cutting all layers with shaped edges. Use of thicker material layers offers the opportunity for faster build rates and/or improved surface finish. We describe our system and present initial experimental results in utilizing tangent-cut layers for object fabrication. Utilizing surface-tangent information introduces new computational complexities in converting CAD descriptions into machine process control commands. We present an algorithm for achieving this conversion, and we illustrate its successful performance.

1 Introduction

CAM-LEM is a Solid Freeform Fabrication process under development through a joint project between Case Western Reserve University and CAM-LEM, Inc. [1,2]. In this process, as is common to all SFF technologies, each part originates from a computer description, which is analyzed and decomposed into boundary contours of thin slices. In CAM-LEM, these individual slices are laser cut from green sheet stock per the computed contours. The resulting part-slice regions are extracted from the sheet stock and stacked to assemble a physical 3-D realization of the original CAD description. The assembly operation includes a lamination procedure that fixes the position of each sheet relative to the preexisting stack and achieves intimate interlayer contact, promoting high-integrity bonding in the subsequent sintering operation. The laminated green object that has been rendered monolithic is then fired to densify the object and control microstructural evolution. The result is a 3-D part which exhibits not only correct geometric form, but functional behavior as well.

One of the problems inherent in all layered manufacturing processes is the stair-cased surface finish resulting from discretization of layers in the build direction. This stair-cased surface finish can be reduced by minimizing the thickness of each layer, but at the expense of fabrication speed. Until now, little effort has be made to interpolate the surface in the build direction.

In [3] we introduced the kinematic theory for a tangential cutting version of the CAM-LEM system; this paper presents recent progress in developing the system described. We have constructed a 5-axis cutting table platform that allows us to laser cut boundary edges tangential to

[1] Department of Electrical Engineering and Applied Physics, Case Western Reserve University.
[2] Department of Mechanical Engineering, Case Western Reserve University.
[3] CAM-LEM, Inc., Cleveland, Ohio, 44108.
[4] Associate Professor, Department of Electrical Engineering and Applied Physics, Case Western Reserve University, Cleveland, Ohio, 44106.

the physical model surface. Tangential cutting enables us to approximate the edge surface with first-order interpolation in the vertical direction, thus eliminating the stair-cased characteristic found in parts made using other RP/SFF technologies.

Several aspects of this approach are discussed here: a description of the hardware used in the system; some initial experimental results in object building with tangent-cut thick layers, and an improved algorithm for generating machine-control commands for tangent cutting from a model's CAD description.

2 Five-axis Tangential Cutting System

The CAM-LEM tangential cutting system, shown in Figure 2.1, is designed to cut successive layers of a part derived from a CAD model description out of sheet material. The system is comprised of three major components: a laser for cutting; a 5-axis cutting table platform for translating and orienting the sheet material relative to the laser; and a material handling robot. The laser is mounted vertically above the 5-axis cutting table. A 4-axis rectilinear robot (to left, not shown) is positioned in front of a platform for loading/unloading sheet material and for selectively gripping and stacking cut contours.

Our 5-axis system consists of 3 translational axes (x,y,z) and two rotational axes (roll and pitch) that position and orient a 6"x 6" cutting table beneath the laser. Sheet material is clamped to the cutting table with vacuum pressure exerted though aluminum honeycomb cells. The cutting table is mounted with an offset 77.5 mm above the intersection of the two rotary axes to maximize clearance with the laser. To achieve the required positions and orientations for cutting the desired tangents about the boundary of a part slice, motion of the x and y axes must be coordinated with the roll and pitch angles of the cutting table. Vertical (z-axis) motion is incorporated in order to keep the material at the laser focal point, at which air ejected from a nozzle helps remove debris and assist cutting.

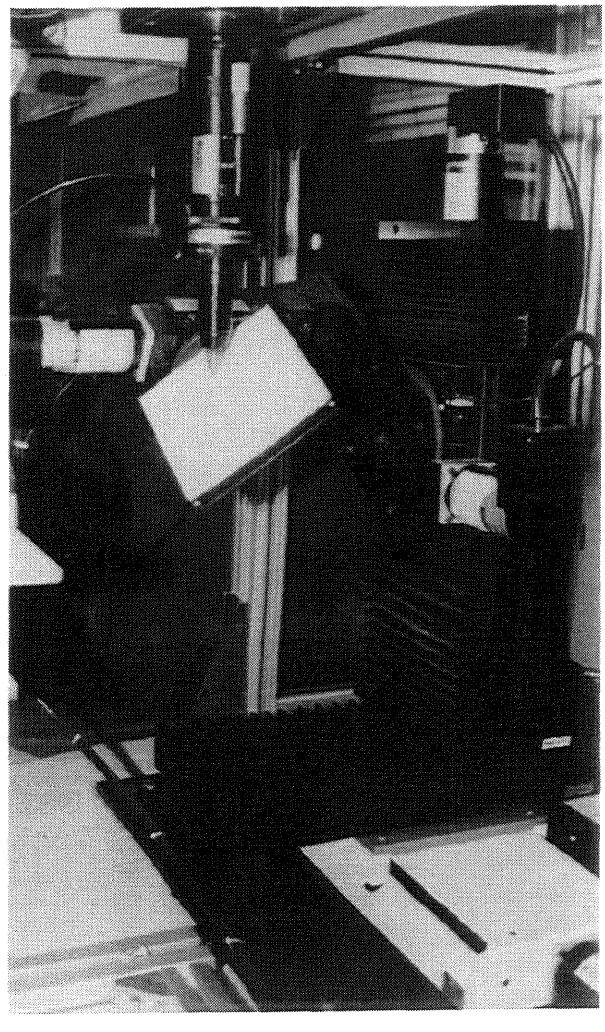

Fig. 2.1: Five-axis tangential cutting system

The maximum orientation angle of the cutting table surface is constrained by the clearance of the laser nozzle such that the pitch and roll axes are limited to ± 73 degrees of motion from vertical during cutting.

Experimental evaluation of the tangent-cutting capability of our system is shown in figures 2.2 and 2.3. Figure 2.2 shows a cross

section of angled cuts made with our system in a sheet of 6mm polystyrene foam. The material was initially oriented such that the laser beam was normal to the material surface. A series of 9 straight 30-mm lines was cut in the material, with the horizontal position increased 7.5mm and the angle increased 9 degrees each step. The final cutting angle tested was 72 degrees. At this final angle, the material thickness cut was 3.2 times deeper than that at normal. As shown, laser cuts in this material were uniform, straight and clean. We are currently investigating angled laser cutting effectiveness in alternative materials, including tape-cast ceramics.

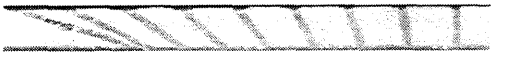

Fig. 2.2: Tangent-cut tests in 6mm polystyrene foam

Figure 2.3 shows an additional test in which the potential value of laser cutting is illustrated. This figure shows two 100-mm diameter spheres constructed from layers of 6mm Styrofoam. On the left, the sphere is approximated with 14 layers of circular cross section and vertical edges. Poor surface approximation is obvious (particularly in regions where the object's tangent plane is nearly horizontal) due to the exaggerated step size of vertical discretization corresponding to thick layers. The sphere on the right in Fig. 2.3 is comprised of 14 tangent-cut layers, each a frustum of a cone. The first and last layers shown required a tangent angle of 55 degrees from vertical. (The top and bottom layers of the sphere are missing, as the required tangent angle of 75 degrees exceeded our system's limit of 73 degrees imposed by kinematic interference.) It is apparent that the tangent-cut thick slices produce a dramatically better surface approximation than normal-cut slices.

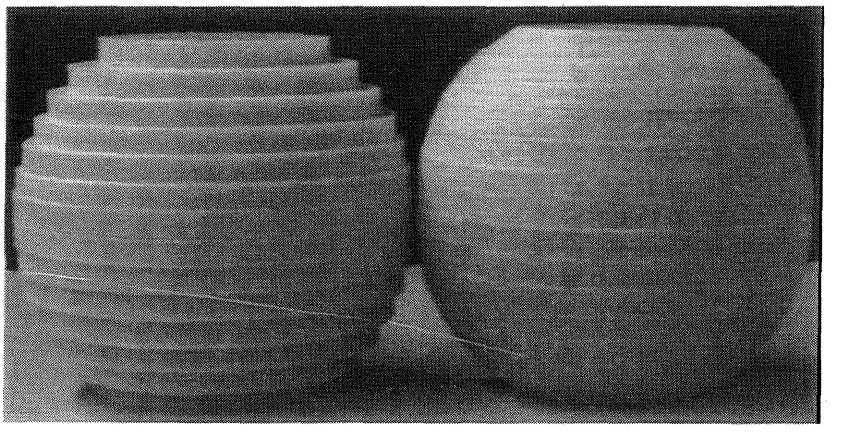

Fig. 2.3: Styrofoam spheres without and with tangential cutting

For the simple example of Fig 2.3, laser-cutting trajectories were computed analytically. To handle an arbitrarily complex part, however, it is necessary to derive kinematically and dynamically feasible laser-cutting trajectories directly from the part's CAD description. This topic constitutes the remainder of this presentation.

3 Trajectory Generation for Tangential Cutting

To exploit the prospective advantages of tangent cutting, it is necessary to deduce machine trajectories from CAD files. Most CAD packages have the ability to compute and report the surface normal or tangent plane at a given point on the surface. Also, files exported in the

ubiquitous STL representation include surface-normal information for every triangular facet. However, this information is not entirely adequate for laser cutting of thick layers. Rather, the relevant constraints for tangent-cutting thick layers are: 1) the contour at the top surface of the thick layer should match the cross section of the CAD model at the corresponding z-height; 2) the contour at the bottom surface of the thick layer should match the corresponding cross section of the CAD model; and 3) both contours must be realizable in terms of a sequence of straight-line segments ("spans") joining points on the top contour to points on the bottom contour.

Our approach is to reduce the edge surface of a layer into a *ruled surface* formed by moving a line (rule) connecting the points on two curves (rails). In considering cutting a layer physically, the contours around the top and bottom surfaces are the rails, and the laser beam is moved as a rule along the contours. Given such a ruled surface, one can deduce the unique inverse kinematics for control of each joint of the cutting platform such that the laser line is directed collinear with the moving rule. An additional important consideration is that the corresponding trajectory should satisfy the constraints of maximum velocity and acceleration of each joint of the laser-cutting system, as well as maximum material removal rate of the laser and maximum laser dwell time (or minimum cutting speed) to avoid excessive burning or melting of the target material.

In this section, we present our method for computing feasible cutting trajectories for realizing good approximations of surface reconstruction in the generation of thick layers.

3.1 Surface Reconstruction from Contours

The problem of surface reconstruction from successive contours is not new. Keppel [4] used triangular facets to stitch successive contours into 3-D layers. He recognized that this problem could be transformed into an equivalent graph-search problem. Fuchs, et. al. [5], analyzed this problem in detail and proposed an optimized search algorithm. Here, we adopt a similar graph-search approach, and modify the result to accommodate the dynamic constraints of the cutting process and of the 5-axis motion. While our approach is extensible to arbitrary contours, we present it for the case of polyline contours, as would result from slicing an STL file.

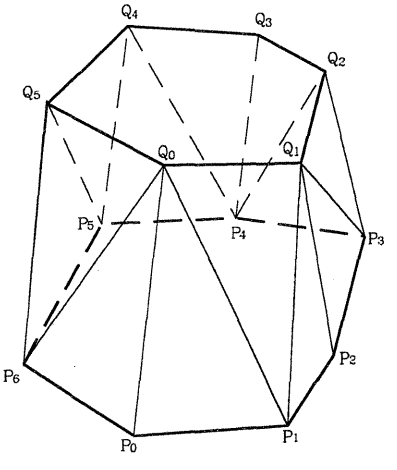

Fig. 3.1 (a): Stitching contours with triangular facets

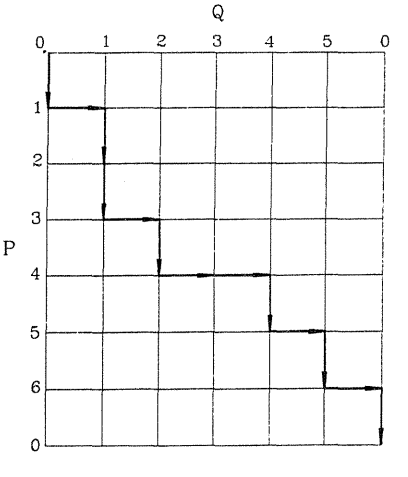

Fig. 3.1 (b): Graph corresponding to the stitching of fig. 3.1 (a)

We presume that successive contours lie in parallel planes, and that each contour is comprised of a sequence of line segments, described by a sequence of points within the respective plane. Figure 3.1 (a) shows an example, in which $(P_0, P_1, ..., P_6)$ represents the bottom contour and $(Q_0, Q_1, ..., Q_5)$ represents the top contour. In Figure 3.1 (a), each segment, such as (P_0, P_1) in the bottom contour or (Q_0, Q_1) in the top contour, is a *contour edge*. Each line that connects the top and bottom contours is a *span*, such as (P_0, Q_0), (P_1, Q_0), (P_1, Q_1) .... Figure 3.1 (b) is the expansion of a directed toroidal graph. Folding the upper edge over to connect with the lower edge forms a cylinder, then joining the left and right edges forms a toroid. In Figure 3.1, each span in (a) is mapped onto (b) as a *graph node*, and each contour edge in (a) is mapped onto (b) as a *graph edge*. In this way, a triangular stitching can be mapped onto the directed graph as a cyclic path that starts and ends at the same node. The path illustrated in Figure 3.1 (b) represents the stitching in Figure 3.1 (a).

Given a pair of contours, there exist $\frac{(m+n)!}{m!n!}$ possible different stitchings where m is the number of points in the bottom contour and n is the number of points in the top contour. Given a criterion to associate a cost with each span (a node in the graph), the surface reconstruction problem can be formulated as a shortest-path search problem in graph theory. Several criteria have been proposed. We have found the "minimum square span length" to be a good cost function. The result is a surface reconstruction between successive layers which is a good approximation to the original surface, and which can, in principle, be created by laser cutting.

3.2 Problems in Faceted Tangential Cutting

While the reconstructed surface illustrated in Figure 3.1 (a) may be a good approximation to the original surface, the use of triangular facets is problematic for trajectory generation. Indeed, it is possible to compute a realizable inverse kinematic trajectory for each of the triangular facets. For example, the facet defined by vertices at (P_0, Q_0, P_1) can be generated by a laser-beam trajectory which is initially collinear with span (P_0, Q_0), then pivots about point Q_0, while tracing out edge (P_0, P_1) of the bottom contour, ending up collinear with span (P_1, Q_0). While this solution is geometrically consistent, it defines a trajectory with excessive dwell time at point Q_0, which is likely unacceptable for laser cutting. In addition, applying the same technique to the next facet, (Q_0, P_1, Q_1), would prescribe pivoting the laser beam about the point P_1 on the bottom contour. The abrupt change from pivoting about a point on the top contour to pivoting about a point on the bottom contour corresponds to a discontinuous velocity reversal of one or both of the orientation axes. Discontinuous velocity changes are physically unachievable; instantaneous velocity reversals, as required to cut typical successive triangular facets, implies an extreme case of a dynamically unsuitable trajectory.

3.3 Trajectory Smoothing in Parameter Space

We can improve upon the trajectory generation implied by the surface reconstruction of Figure 3.1 by further interpreting the graph of Figure 3.1(b). This graph represents an abstraction of the surface reconstruction problem, and a graph search applied to this representation resulted in the path shown in Figure 3.1(b), defining the surface reconstruction of Figure 3.1(a). We next re-associate the abstract graph of Figure 3.1(b) with physical dimensions by interpreting the Q axis as the path length along the top contour, and the P axis as the path length along the bottom contour. We introduce the new variables u_t and u_b to be path-length variables, ranging from 0 to

1, defining the fractional completion of the traversal of the top and bottom contours, respectively. The dimensionless graph of Q vs. P of Figure 3.1(b) is translated to a graph in u_t vs. u_b, rescaled such that each graph edge of Figure 3.1(b) is assigned a length proportional to the length of the corresponding contour segment. The resulting plot is the path-length distance along the top contour vs. path-length distance along the bottom contour. This plot defines the motion of end-points of a span sweeping out the ruled surface joining the top contour to the bottom contour.

From this viewpoint, the dynamics problem of velocity reversals at facet boundaries is apparent. A horizontal path segment in u_t vs. u_b indicates zero velocity of u_b, corresponding to the laser line pivoting about a point in the bottom contour. Similarly, vertical path segments in u_t vs. u_b indicate pivoting about a point on the top contour. Path segments sequencing from vertical to horizontal (or vice versa) indicate velocity reversals in orientation. In the parameter space u_t vs. u_b we can see that the ideal path, with respect to a smooth dynamic trajectory and constant laser cutting speed, would be a 45-degree line from $(u_b, u_t) = (0,0)$ to $(u_b, u_t) = (1,1)$. In contrast, the ideal path with respect to optimized surface reconstruction, without regard to cutting or motion dynamics, consists entirely of vertical and horizontal segments. To achieve good surface reconstruction with consideration of dynamic constraints, we spatially low-pass filter the computed path in u_t vs. u_b to produce a smoothed path. This smoothed path constitutes an approximation to the computed, faceted surface reconstruction, but it eliminates the rapid velocity changes corresponding to the transitions between the computed facets.

In practice, we low-pass filter u_t vs. u_b by defining separate functions of time, $u_t(t)$ and $u_b(t)$. These functions are initially derived from the computed graph of u_t vs. u_b, then low-pass filtered to produce smoothed path-length vs. time functions. The resulting smoothed functions define endpoints of a moving span between the top and bottom contours. At each instant in time, the coordinates of these endpoints can be computed, and the corresponding inverse kinematics for the laser cutter yields an unambiguous solution for control of the 5-axis system.

Our smoothing approach redefines the surface between the top and bottom contours, smoothing over discrete changes in surface normal. However, discrete changes in surface normal are sometimes deliberate (e.g., in defining the faces of a cube) rather than artifacts of reconstruction. When it is desired to preserve a particular span (e.g., the edge of a cube) identically, we can do so by defining the corresponding values of u_t and u_b to be constant vs. time in the definitions of $u_t(t)$ and $u_b(t)$ for a duration exceeding the time constant of our low-pass filter. The result will produce a graph of u_t vs. u_b that includes the desired span.

3.4 Illustration of Trajectory Smoothing in Parameter Space

Here we illustrate the surface reconstruction and trajectory smoothing technique with a realistically complex example. Figure 3.2 (a) is the wire frame display of a layer edge surface reconstructed with the triangular stitching algorithm described in section 3.1. Contour data comes from two sections of an STL model of a human head. The top contour has 344 segments and the bottom contour has 345 segments.

Figure 3.2 (b) shows the span trajectory smoothed with our spatial filter. First, we defined discretized functions $u_t(t)$ and $u_b(t)$ using 1200 samples of u_t and u_b. A moving central-

average filter of window width 19 was applied to both series $\{u_t\}$ and $\{u_b\}$. Comparing Figures 3.2 (b) to (a) shows the effect of our smoothing algorithm. An attempt to cut the layer defined by Figure 3.2(a) would result in slow execution, poor tracking, and excessive laser-induced ablation at pivot points. The layer defined by Figure 3.2(b) yields a well-behaved trajectory specification, as well as a smoother surface reconstruction. Note, though, that the top and bottom contours, respectively, of the two models (3.2(a) and 3.2(b)) are identical. The smoothing algorithm does not distort the part boundaries at the slice planes. Thus, layers constructed with smoothed surfaces can be expected to mate identically with the layers immediately above and below within a stacked assembly comprising a 3-D part (e.g., as in Fig 2.3).

At the time of this writing, our trajectory smoothing algorithm has not yet been incorporated into the control of our new 5-axis platform. Surface reconstruction and smoothing is currently performed off line. To reduce the size of datafiles required to drive the laser cutter, surface reconstruction and smoothing is being converted to an on-line process, computed during cutting.

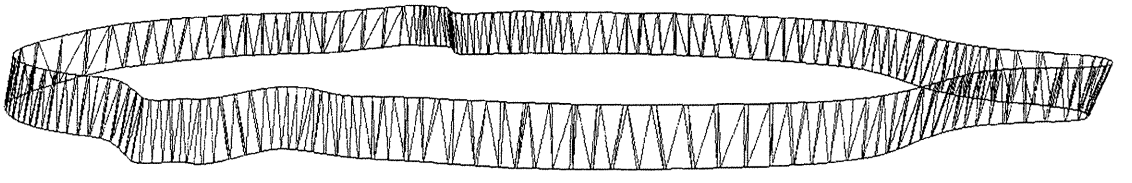

Fig. 3.2 (a): Span trajectory from surface reconstruction

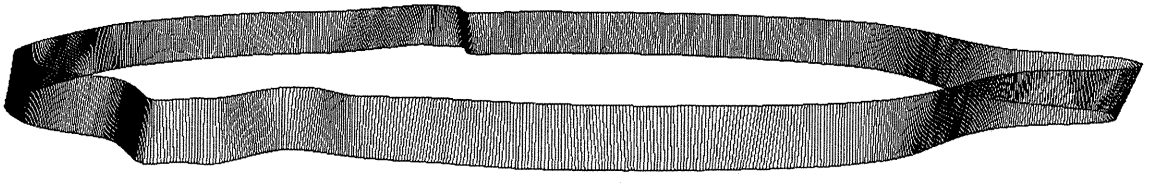

Fig. 3.2 (b): Smoothed span trajectory

4 Discussion and Conclusion

The work in progress presented in this paper has demonstrated the feasibility of extending the CAM-LEM technique to the fabrication of components using tangent cutting to optimize surface finish and build time. The current capabilities and limitations of our experimental 5-axis laser-cutting system were illustrated, and the potential for improving build rate and/or surface quality was demonstrated with a simple physical example fabricated with our system.

A significant challenge encountered in our research has been the derivation of a suitable laser-cutting trajectory from CAD information. While CAD models typically incorporate sufficient information to specify the surface tangent planes at arbitrary surface points, such information is not adequate for generating cutting-trajectory profiles. Instead, an optimal surface approximation must be computed, based on a sequence of line-segment spans connecting top and

bottom boundaries of a layer. In addition to achieving a good approximation to the original surface, the surface reconstruction algorithm must also result in a kinematically and dynamically desirable laser-cutting trajectory. We have presented an algorithm which accomplishes this for contours consisting of polylines, as is the case for slices of models stored in the STL format.

In continuing work, we are extending our surface-reconstruction and smooth trajectory-generation algorithm to work with non-polygonal contours, including arcs and NURBS. Further, this algorithm is being converted to a real-time process to be executed during laser cutting. On-line translation of CAD models to cutting trajectories will permit use of more compact data files while offering improved resolution.

Initial tests of angular laser cutting of materials has been encouraging. However, we have seen that the maximum practical cutting angle can be restrictive for some materials. Laser-cutting parameters, including cutting speed, laser power, air-jet effects, and laser optics, will have to be explored for optimizing cutting quality for materials of interest for CAM-LEM processing.

References

[1] B. B. Mathewson, W. S. Newman, A. H. Heuer, and J. D. Cawley, "Automated Fabrication of Ceramic Components from Tape-Cast Ceramic," in *Solid Freeform Symposium Proceedings*, University of Texas at Austin Publishers, Austin, TX, August, 1995.

[2] J. D. Cawley, Z. Liu, W. S. Newman, B. B. Mathewson, A. H. Heuer, "Al_2O_3 Ceramics Made by CAM-LEM Technology," *Solid Freeform Symposium Proceedings*, University of Texas at Austin Publishers, Austin, TX, August, 1995.

[3] W. Newman, Y. Zheng, and C. C. Fong, "Trajectory Generation from CAD Models for Computer-Aided Manufacturing of Laminated Engineering Materials," *in Proceeding of the 26th International Symposium on Industrial Robots*, pp. 153-158, Singapore, October 4-6, 1995.

[4] E. Keppel, "Approximating Complex Surfaces by Triangulation of Contour Lines," *IBM J. Res. Dev.*, 19:2-11, January 1975.

[5] H. Fuchs. A. M. Kedem, and S. P. Uselton, "Optimal Surface Reconstruction from Planar Contours," *Commun. ACM*, 20:693-702, October 1977.

Acknowledgements

The authors wish to thank Ting-Chu Ko, Department of Materials Science and Engineering, CWRU, for experimental assistance in the performance of this work. The authors also thank Professors J. D. Cawley and A. H. Heuer, also of CWRU's MSE Department, for numerous technical discussions contributing to this research. This work was supported by National Science Foundation grant DMI94-20373, by NSF Young Investigator Award number IRI92-57269, and by ONR grant N00014-95-10107. This support is gratefully acknowledged.